Hybrid statistical–dynamical seasonal prediction of summer extreme temperatures in Europe

SUPPORTING INFORMATION

Luca Famooss Paolini [a], Paolo Ruggieri [a], Salvatore Pascale [a], Erika Brattich [a], Silvana Di Sabatino [a]

[a] *Department of Physics and Astronomy "Augusto Righi", University of Bologna, Bologna, Italy*

Corresponding author: Luca Famooss Paolini, luca.famoosspaolini@unibo.it

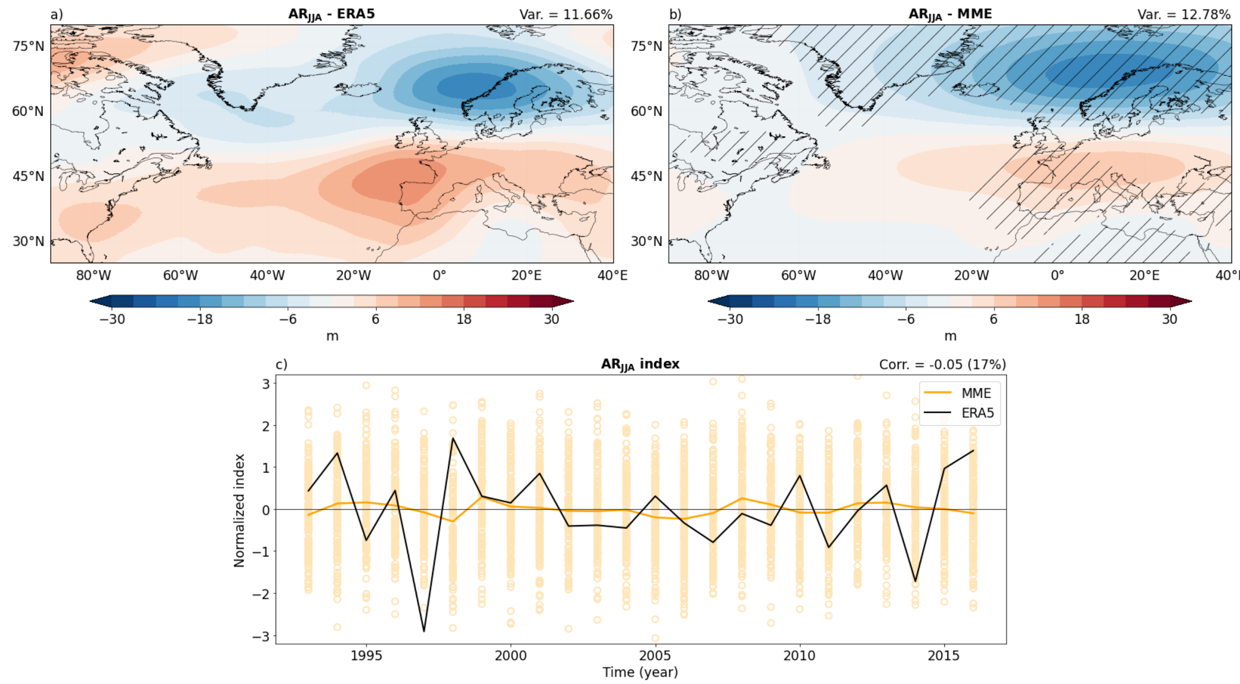

FIG. S1. a) Summer (JJA) Atlantic Ridge pattern, calculated as the third EOF of summer Z500 over the North Atlantic sector (25°–80°N, 90°W–40°E) in ERA5. The variance of the summer low-frequency atmospheric variability explained by the Atlantic Ridge is shown on the top right of the subplot. b) As a) but in the C3S MME. Refer to section 2 for more details about the EOF analysis applied to the C3S MME. The results about the C3S MME are represented as MME mean. Hatched areas represent the regions with consistent sign in Z500 anomalies associated with the Atlantic Ridge across all SPSs. c) The summer Atlantic Ridge index in ERA5 (black) and in the C3S MME (orange). The correlation between the summer Atlantic Ridge index in ERA5 and the corresponding index as ensemble mean of the MME is presented on the top right of the subplot, along with its confidence level enclosed in parentheses.

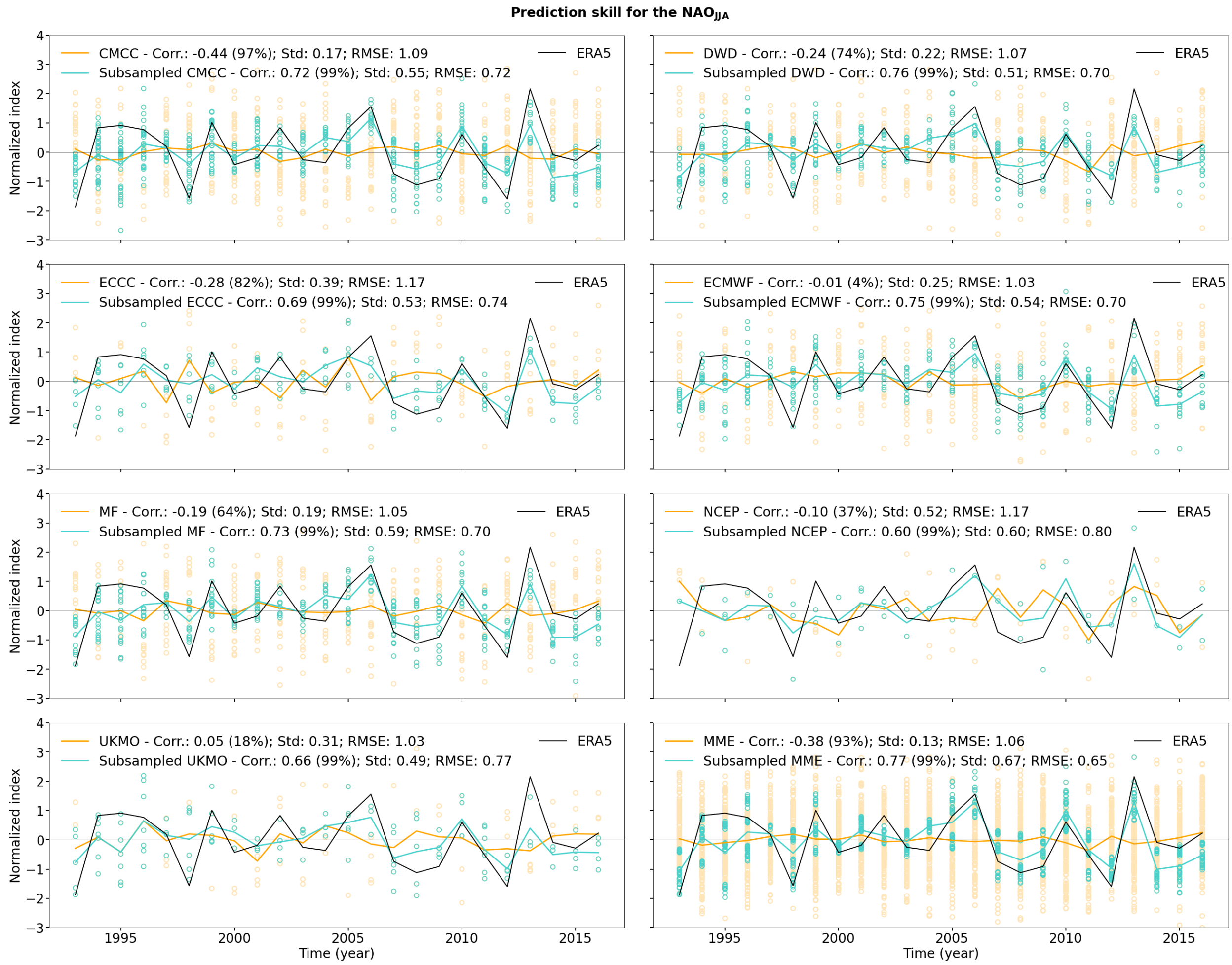

FIG. S2. The summer NAO index in ERA5 (black) and in the individual full (orange) and subsampled (azul) C3S SPS ensembles. The orange (azul) circles represent each members of the individual full (subsampled) C3S SPS ensemble. The orange (azul) solid lines represents the ensemble mean of the full (subsampled) C3S SPS enseble. The subsampling of the individual SPS ensembles is performed using all the April NAO predictors. Specifically, 10, 7, 3, 6, 6, 1, and 5 members are selected for every predictor for the CMCC, DWD, ECCC, ECMWF, MF, NCEP and UKMO SPSs, respectively. The correlation between the summer NAO index in ERA5 and the corresponding index as ensemble mean in the full and subsampled SPS ensemble is presented in the legend, along with its confidence level enclosed in parentheses. The variability of the summer NAO index as ensemble mean of the full and subsampled SPS ensemble is also shown in the legend as standard deviation (std). Finally, the RMSE of the full and subsampled MME mean NAO index computed with respect to the summer NAO index in ERA5 is shown at the end of the legend. The plot in the bottom right is the same as above, but for the full and subsampled MME. In this case, the subsampling is performed selecting 10 members for every April predictor.

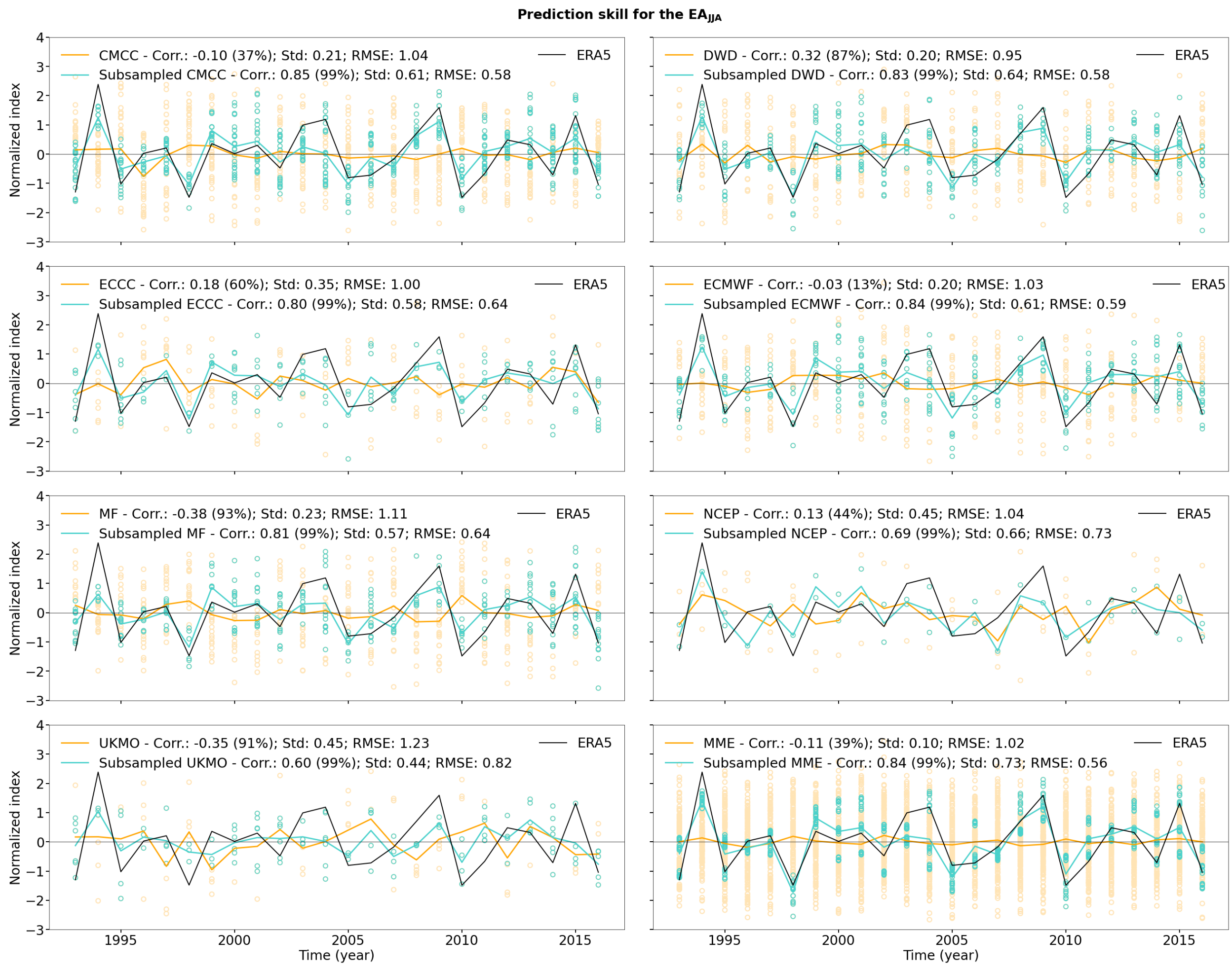

FIG. S3. Same as Figure S2, but performing the subsampling of the individual SPS ensembles and MME using all the April EA predictors.

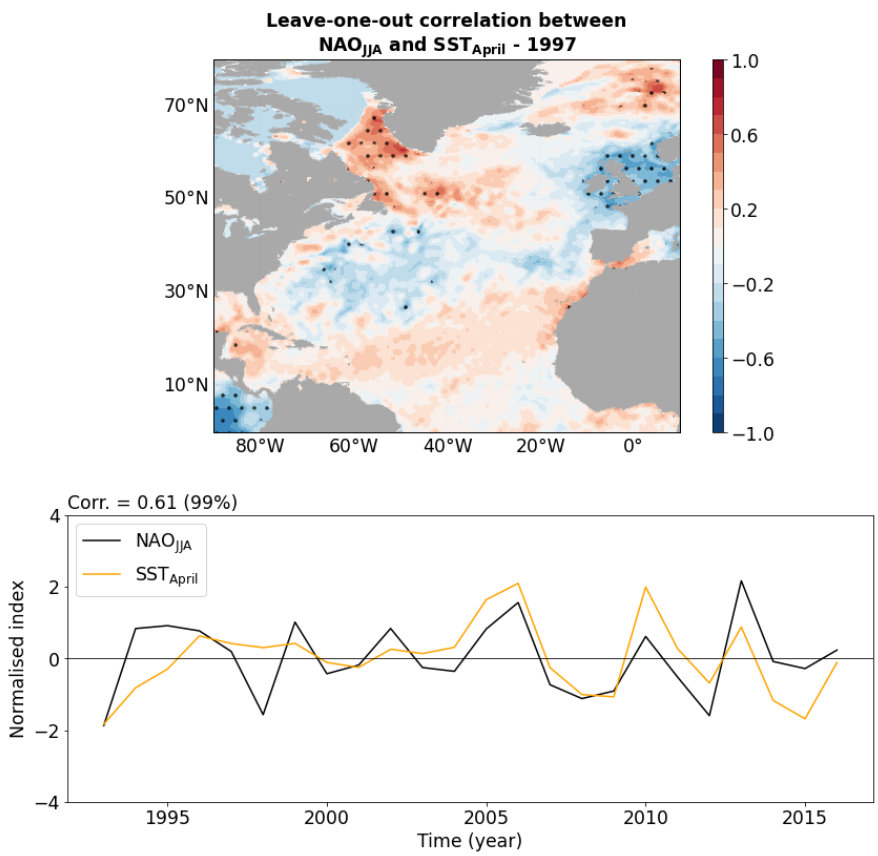

1-year out	Correlation
1993	0.54
1994	0.66
1995	0.64
1996	0.6
1997	0.61
1998	0.67
1999	0.61
2000	0.61
2001	0.61
2002	0.61
2003	0.61
2004	0.62
2005	0.6
2006	0.55
2007	0.61
2008	0.59
2009	0.59
2010	0.62
2011	0.62
2012	0.6
2013	0.6
2014	0.63
2015	0.63
2016	0.61
Min	0.54
Mean	0.61
Max	0.67
3-year out	**Correlation**
Min	0.43
Mean	0.54
Max	0.61

FIG. S4. (top) Leave-one-out cross-validated correlation (shadings) between the summer NAO index and the April sea surface temperature (SST) in the North Atlantic (90°W–10°E; 0°–80°N), using ERA5 data. The year 1997 is here shown as an example and it has been randomly selected within the time period 1993–2016. Black dots denote correlations that are statistically significant at the 90% confidence level. (bottom) The summer NAO (black) and April SST (orange) indices. Refer to section 2 in the manuscript for more details about the calculation of the April NAO predictor index. The correlation between the two indices is provided in the top right corner, along with its confidence level enclosed in parentheses. (left) Leave-one-out and leave-three-out cross-validated correlation between the summer NAO and April SST indices.

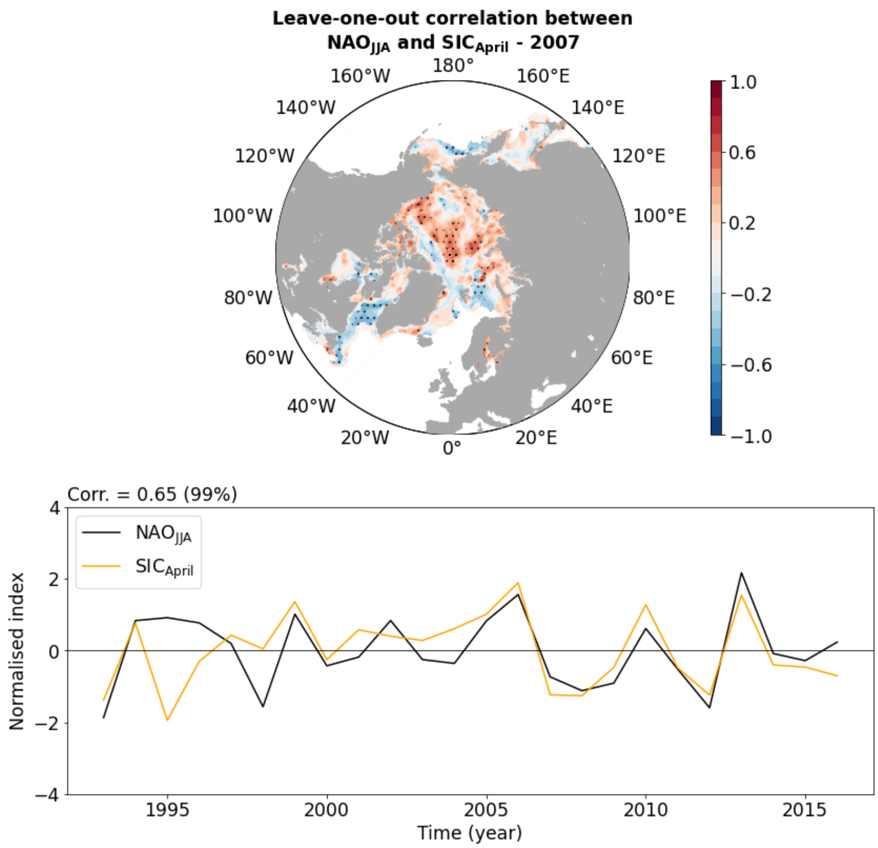

1-year out	Correlation
1993	0.61
1994	0.64
1995	0.81
1996	0.67
1997	0.65
1998	0.69
1999	0.63
2000	0.65
2001	0.66
2002	0.64
2003	0.65
2004	0.66
2005	0.63
2006	0.6
2007	0.64
2008	0.62
2009	0.64
2010	0.64
2011	0.64
2012	0.62
2013	0.59
2014	0.65
2015	0.65
2016	0.66
Min	0.59
Mean	0.65
Max	0.81
3-year out	**Correlation**
Min	0.52
Mean	0.61
Max	0.81

FIG. S5. Same as Figure S4, but for the sea-ice concentration (SIC) in the Northern Hemisphere (north of 40°N).

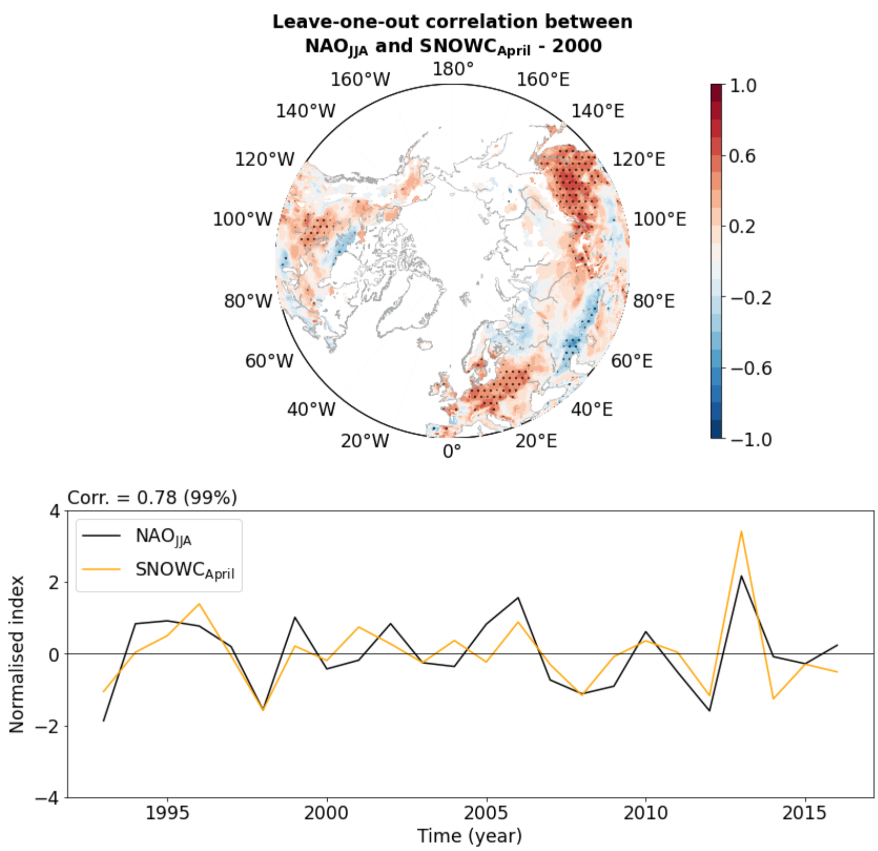

1-year out	Correlation
1993	0.77
1994	0.79
1995	0.77
1996	0.77
1997	0.78
1998	0.75
1999	0.78
2000	0.78
2001	0.79
2002	0.78
2003	0.77
2004	0.79
2005	0.8
2006	0.77
2007	0.78
2008	0.76
2009	0.79
2010	0.77
2011	0.78
2012	0.76
2013	0.72
2014	0.8
2015	0.77
2016	0.79
Min	0.72
Mean	0.78
Max	0.8
3-year out	**Correlation**
Min	0.67
Mean	0.76
Max	0.79

FIG. S6. Same as Figure S4, but for the snow cover (SNOWC) in the Northern Hemisphere (north of 40°N).

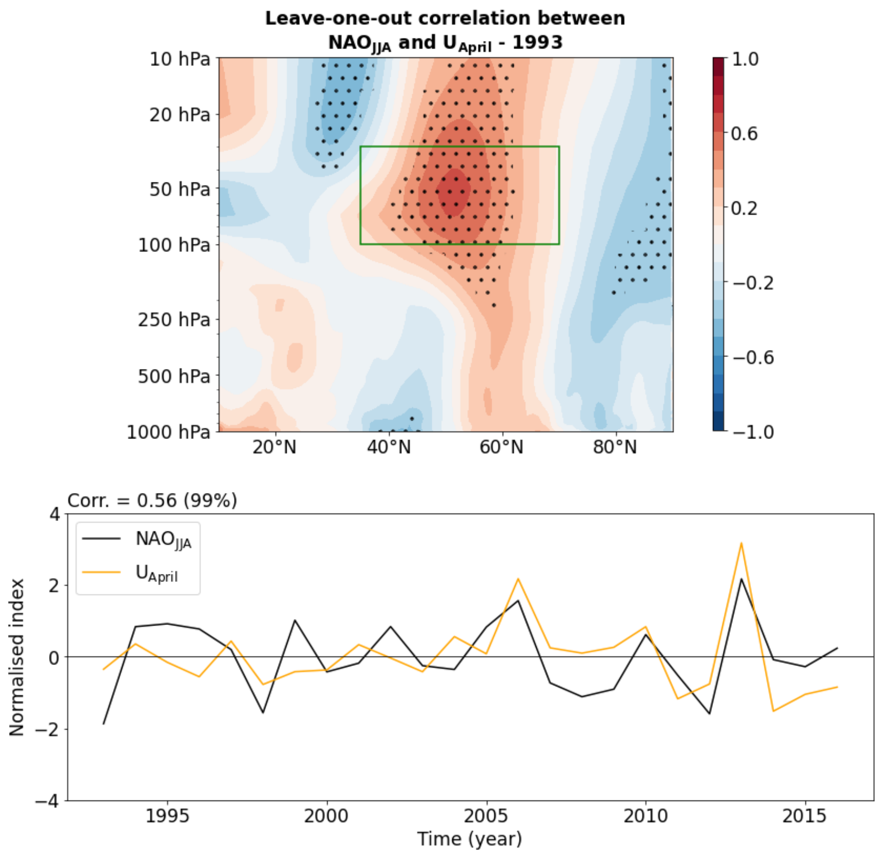

1-year out	Correlation
1993	0.58
1994	0.56
1995	0.58
1996	0.6
1997	0.56
1998	0.55
1999	0.6
2000	0.56
2001	0.57
2002	0.58
2003	0.56
2004	0.58
2005	0.57
2006	0.5
2007	0.58
2008	0.59
2009	0.59
2010	0.56
2011	0.56
2012	0.55
2013	0.4
2014	0.59
2015	0.57
2016	0.58
Min	0.4
Mean	0.56
Max	0.6
3-year out	**Correlation**
Min	0.35
Mean	0.56
Max	0.63

FIG. S7. Same as Figure S4, but for the zonal wind (U). The zonal wind is zonally-averaged over the longitudinal range of the North Atlantic sector as in Wang and Ting (2022) (75°W–15°E). The green box represents the part of the lower stratosphere where the zonally-averaged zonal wind is averaged to define the April U index shown in the plot on the bottom (orange line; 30 hPa–100 hPa; 35°N–70°N).

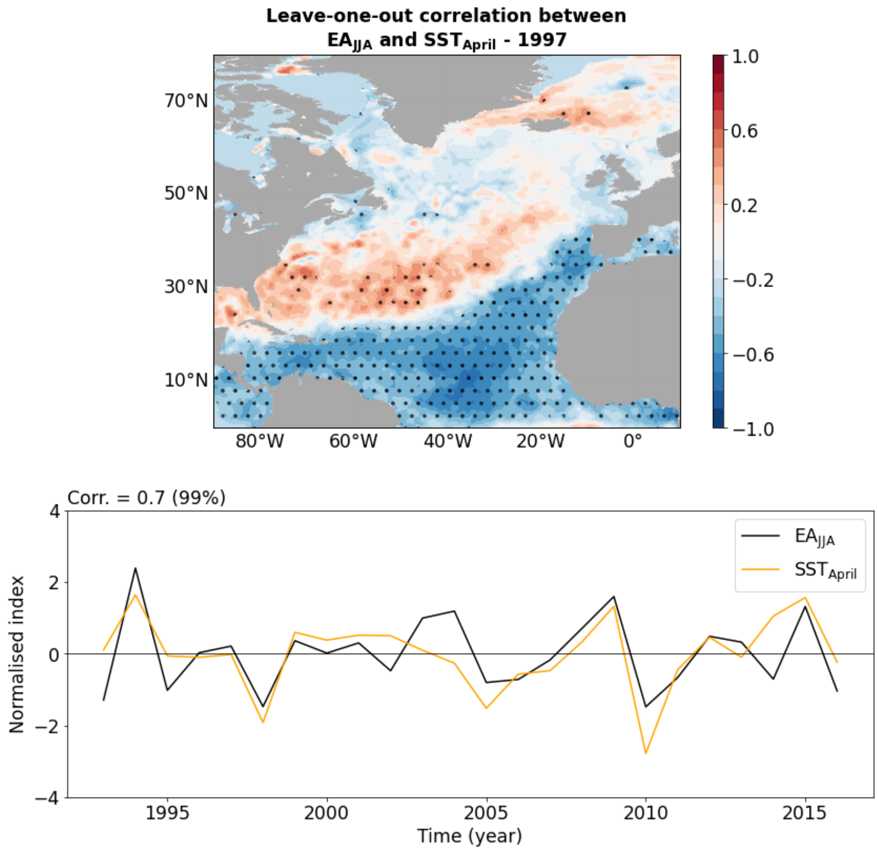

1-year out	Correlation
1993	0.73
1994	0.65
1995	0.71
1996	0.7
1997	0.7
1998	0.66
1999	0.7
2000	0.7
2001	0.7
2002	0.72
2003	0.71
2004	0.74
2005	0.69
2006	0.7
2007	0.7
2008	0.7
2009	0.67
2010	0.67
2011	0.7
2012	0.7
2013	0.7
2014	0.76
2015	0.67
2016	0.71
Min	0.65
Mean	0.7
Max	0.76
3-year out	**Correlation**
Min	0.63
Mean	0.7
Max	0.77

FIG. S8. (top) Leave-one-out cross-validated correlation (shadings) between the summer EA index and the April sea surface temperature (SST) in the North Atlantic (90°W–10°E; 0°–80°N), using ERA5 data. The year 1997 is here shown as an example and it has been randomly selected within the time period 1993–2016. Black dots denote correlations that are statistically significant at the 90% confidence level. (bottom) The summer EA (black) and April SST (orange) indices. Refer to section 2 in the manuscript for more details about the calculation of the April EA predictor index. The correlation between the two indices is provided in the top right corner, along with its confidence level enclosed in parentheses. (left) Leave-one-out and leave-three-out cross-validated correlation between the summer EA and April SST indices.

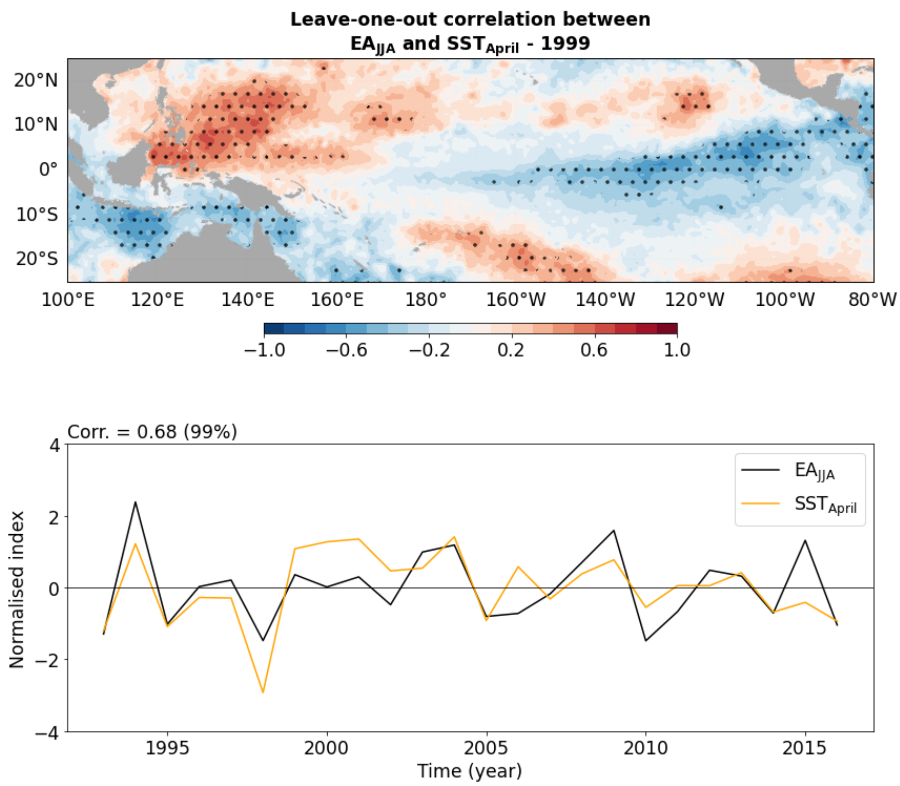

1-year out	Correlation
1993	0.66
1994	0.66
1995	0.67
1996	0.68
1997	0.69
1998	0.66
1999	0.68
2000	0.71
2001	0.69
2002	0.7
2003	0.68
2004	0.66
2005	0.67
2006	0.71
2007	0.68
2008	0.68
2009	0.68
2010	0.68
2011	0.69
2012	0.68
2013	0.68
2014	0.68
2015	0.74
2016	0.67
Min	0.66
Mean	0.68
Max	0.74
3-year out	**Correlation**
Min	0.62
Mean	0.69
Max	0.75

FIG. S9. Same as Figure S8, but for the SST in the tropical Pacific (100°E–80°W; 25°S–25°N).

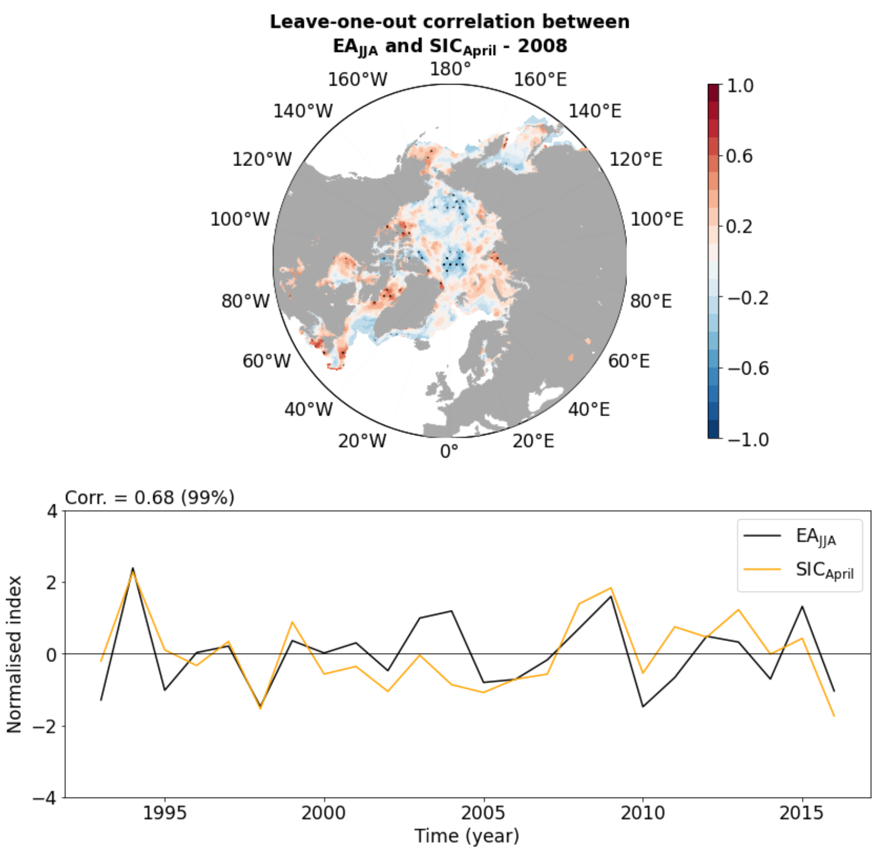

1-year out	Correlation
1993	0.69
1994	0.58
1995	0.7
1996	0.68
1997	0.68
1998	0.64
1999	0.68
2000	0.68
2001	0.69
2002	0.68
2003	0.69
2004	0.76
2005	0.67
2006	0.67
2007	0.68
2008	0.67
2009	0.63
2010	0.68
2011	0.71
2012	0.67
2013	0.68
2014	0.68
2015	0.68
2016	0.66
Min	0.58
Mean	0.68
Max	0.76
3-year out	**Correlation**
Min	0.58
Mean	0.66
Max	0.76

FIG. S10. Same as Figure S8, but for the SIC in the Northern Hemisphere (north of 40°N).

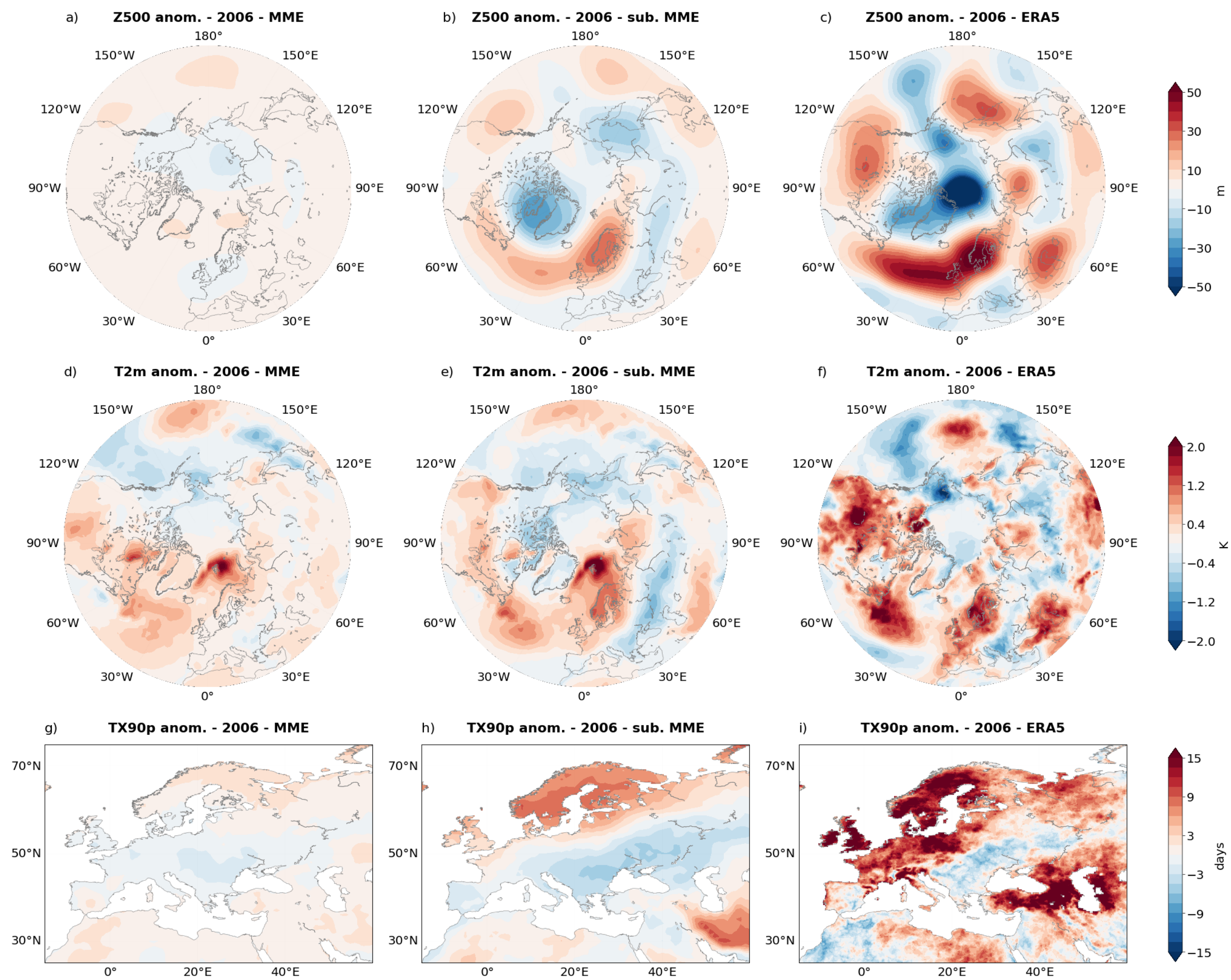

FIG. S11. a) Z500 anomalies (m) for the full C3S MME mean during summer 2006. b) As a) but for the subsampled C3S MME mean. The subsampling of the MME is performed using all the April EA predictors computed with the leave-three out cross-validation procedure and selecting 10 members for every predictor. c) As a) but for ERA5. d, e, f) As a, b, c) but for T2m (K). g, h, i) As a, b, c) but for TX90p (days).

References

Wang, L., and M. Ting, 2022: Stratosphere-Troposphere Coupling Leading to Extended Seasonal Predictability of Summer North Atlantic Oscillation and Boreal Climate. *Geophysical Research Letters*, **49 (2)**, e2021GL096 362.